

RSC Advances



This is an *Accepted Manuscript*, which has been through the Royal Society of Chemistry peer review process and has been accepted for publication.

Accepted Manuscripts are published online shortly after acceptance, before technical editing, formatting and proof reading. Using this free service, authors can make their results available to the community, in citable form, before we publish the edited article. This *Accepted Manuscript* will be replaced by the edited, formatted and paginated article as soon as this is available.

You can find more information about *Accepted Manuscripts* in the [Information for Authors](#).

Please note that technical editing may introduce minor changes to the text and/or graphics, which may alter content. The journal's standard [Terms & Conditions](#) and the [Ethical guidelines](#) still apply. In no event shall the Royal Society of Chemistry be held responsible for any errors or omissions in this *Accepted Manuscript* or any consequences arising from the use of any information it contains.

Solution-blown Core-shell Hydrogel Nanofibers for Bovine Serum Albumin Affinity Adsorption

Junying Tong^a, Xianlin Xu^{a,*}, Hang Wang^a, Xupin Zhuang^{a,b,*},
and Fang Zhang^a

^a College of Textile, Tianjin Polytechnic University, Tianjin 300387, P.R.China

^b Key Laboratory of Advanced Textile Composite Materials of Ministry of Education,
Tianjin Polytechnic University, Tianjin300387, P.R.China

ABSTRACT

In this work, nylon 6 core-chitosan/poly (vinyl alcohol) (PVA) shell hydrogel nanofibers (NCNFs) were fabricated by coaxial solution blowing. The hydrogel fibers were 80–650 nm in diameter with smooth surfaces. These fibers were distributed randomly and formed three-dimensional mats. Cibacron Blue F3GA (CB) was then immobilized onto the membrane surfaces for subsequent protein affinity adsorption. The amount of PVA in the shell greatly influenced CB content and bovine serum albumin (BSA) adsorption. The highest BSA adsorption capacity achieved by the NCNF membranes with immobilized CB was 379.43 mg/g. Results showed that NCNFs combine the large capacity of hydrogels and the high flux of nanofibrous mats for affinity adsorption.

Keywords: Nanofiber; Affinity adsorption; Solution blowing; Core-shell; Hydrogel

* E-mail address: xianlinxu@163.com(X.L.Xu); zhxupin@tjpu.edu.cn(X.P.Zhuang); Fax: +86-22-83955287; Tel: +86-22-83955002

1. Introduction

Affinity chromatography is an important method because of its wide application in protein separation and purification. It is usually carried out in packed-bed chromatography columns filled with soft gels¹. However, the classical bead-based column chromatography exhibits drawbacks such as slow intraparticle diffusion, large pressure drop through the column, low product throughput and high cost, and etc.¹⁰. With the development of membrane technology, ligand molecules are introduced into the surfaces of membrane to specifically capture ligate, while letting other molecules to pass through. Affinity membrane chromatography is a new type of separation method that offers some apparent advantages over conventional bead-packed column chromatography, which combining membrane use and affinity chromatography. These advantages include higher flow rate, shorter diffusion path, lower pressure drop, and simple scale-up process²⁻⁴. However, affinity membrane chromatography have to face the negative effect of decreasing target molecule adsorption capacity because that binding can only take place on the surface of the membrane and the membranes have limited superficial area.

Nanofiber membranes have recently received increased attention in terms of their use in the separation of analytes on account of their porous structure, large surface area, and low production cost. With their extremely large surface areas, nanofiber membranes can increase the chances of contact of target molecules to the fiber surface. In this regard, the binding capacity of ligands is greatly augmented relative to that of flat and hollow membranes⁵⁻⁷. Furthermore, nanofiber membranes show high porosity,

which improves filtration efficiency⁸⁻¹². Hence, nanofiber membranes have been extensively developed as affinity membranes. Zhang¹³ successfully electrospun hybrid chitosan/nylon-6 nanofibrous mats and immobilized Cibacron Blue F3GA (CB) on these mats as the affinity ligand. Ma¹⁴ prepared a protein A/G functionalized electrospun regenerated cellulose (RC) nanofiber mesh as an affinity membrane for immunoglobulin G (IgG) purification.

Solution blowing is a new nanofiber fabrication method that uses high-speed airflow as driveforce. Compared with electrospinning, solution blowing presents significant advantages such as high productivity, easy accessibility and low energy consumption¹⁵⁻¹⁹. Besides their high specific surface areas, solution-blown nanofibers are commonly curled in three-dimension because of the effect of turbulent flow in the gas flow field. This configuration enhances the transport property of the material²⁰, and hence makes the solution-blown nanofiber a good candidate for affinity adsorption.

On the other hand, the mechanism of protein adsorption onto a surface is highly complex, and the interaction depends on the physicochemical properties of the surface like the surface area, topography, hydrophobicity/ hydrophilicity, electrostatic charges, polar/nonpolar groups, chemical structure and the properties of the protein itself²¹. In recent years, a great deal of interest has been observed in relation to the applicability of hydrogels as adsorbents²²⁻²³, on account of their form of three-dimensional cross-linked polymer networks of flexible chains, which are able to absorb and retain water and solute molecules.

In our previous work, a novel hydrogel nanofiber membrane was fabricated via solution blowing of chitosan and poly (vinyl alcohol) (PVA) solution²⁴ with ethylene glycol diglycidyl ether (EGDE) as the cross-linker. The chitosan/PVA nanofiber membranes show the combined advantages of hydrogel and nanofibrous membranes. Over here, chitosan and its derivatives are excellent adsorbents since chitosan is positively charged in the mild acidic and near neutral pH conditions while many proteins are negatively charged^{23,25}. On the other hand, PVA can better react with Bovine Serum Albumin, and often used in protein adsorption material²⁶. Furthermore, PVA could greatly improve the effective utilization of affinity binding sites because of its water absorption and swelling properties. Thus, the chitosan/PVA hydrogel nanofiber could be expected to be an advanced membrane with good performance in affinity adsorption on account of its large capacity and high flux.

In this study, a core-shell nanofiber, with chitosan/PVA as shell and nylon 6 as core, was fabricated to investigate its affinity adsorption performance. The chitosan/PVA shell is designed as adsorption layer, and the nylon 6 core is designed to improve its mechanical property and spinnability. CB and bovine serum albumin (BSA) were selected as ligand-ligand research models to test adsorption activity. The structure and properties of the solution-blown hydrogel nanofiber mats, including the ratio of core-shell content, different contents of chitosan and PVA, the change of degree of crosslinking, pH value and the initial concentration of the protein solution, were characterized and the CB functionalized membranes were studied in terms of BSA capturing abilities.

2. Experimental

2.1. Materials and preparation

Chitosan, with viscosity-average molecular weight of 5.1×10^4 and deacetylation degree of 0.92, was provided by Zhejiang Ao-Xing Biotechnology Co. Ltd. (Zhejiang, China). PVA, with the degree of hydrolyzation of 97 mol%, was purchased from Tianjin Guangfu Fine Chemical Research Institute (Tianjin, China). EGDE (medical grade) was purchased from Shanghai YiBo Bio-Pharmaceutical Tech. Co., Ltd. (Shanghai, China) and used as a water soluble cross-linker. Analytical-grade formic acid (88 wt%) was used as-received. CB (reagent grade) was purchased from Dalian MeiLun Bio-Pharmaceutical Tech. Co., Ltd. (Dalian, China) and used as the ligand.

The shell spinning solution was produced by dissolving chitosan and PVA in formic acid to a total polymer mass fraction of 4 wt%, with EGDE blended into the mixture before spinning. The core solution was composed of 16 wt% nylon-6 in formic acid.

2.2. Coaxial solution blowing of nanofibers

A purpose-built coaxial solution blowing setup, was used for the experiments. The spinning program may be described briefly as follows: The nylon-6 solution and chitosan/PVA solution were respectively fed to the inner and outer orifices of the coaxial spinneret, and the compressed air was supplied to a coaxial outer slot. After the solution streams were pressed out of the orifices, they were stretched to extreme lengths by the high-velocity gas flow. The nanofibers formed along with solvent evaporation and deposited on a porous collector (the collector distance was 60 cm) to form a fibrous mat. Finally, the produced nanofiber mats were heat-treated in a

vacuum oven at 60 °C for 3 h to enhance the cross-linking reaction and to remove the residual formic acid.

The coaxial spinneret used in this study has inner and outer orifices measuring 0.5 and 0.8 mm in diameter, respectively. The width of the coaxial air slot was 1.0 mm, and the drawing gas flow was supplied at 0.15 MPa. The resultant nylon-6 core–chitosan/PVA shell nanofibers are denoted as NCNFs, and the samples with different content ratios are given in Table.1.

2.3. CB immobilization

CB (50 mg) was dissolved in 50 mL of water, and the dye solution was heated to 60 °C, followed by addition of 30 mg of NCNFs. After soaking for 30 min, 25 wt% sodium chloride (NaCl) was added to the mixture. The temperature was maintained at 60 °C for 30 min. Then, 2.5 mL of 25 wt% Na₂CO₃ solution was added, and the reaction temperature was increased to 80 °C for another 4 h. The modified nanofibrous membranes were washed thoroughly with warm water and methanol until no CB molecules were detected in the washing solution by UV-vis absorbance measurement. The reaction of chitosan/PVA with CB was confirmed by Fourier transform infrared spectroscopy (FTIR; Nicolet 6700, USA). The CB loading on the nanofibrous membranes was determined in terms of sulfur content using elemental analysis (EA).

2.4. Characterization of nanofibrous membranes

The morphology of the nanofiber mats was observed using field emission–scanning electron microscopy (FE–SEM, Hitachi S-4800). All specimens were coated with a

conductive layer of sputtered gold, and fiber diameters were determined as mean values of 50 measurements on the FE–SEM images. The core–shell structures of the fibers were confirmed through transmission electron microscopy (TEM, Hitachi H–7650).

2.5. BSA adsorption studies

BSA adsorption capacities of the CB attached to the NCNFs were measured under different concentrations, adsorption times, and pH values of the adsorption media. PBS was used to prepare the adsorption media with different pH values. In a typical adsorption test, 10 mg of the NCNFs was combined with 10 mL of the BSA solution for certain time at 30 °C, followed by extensive washing with distilled water. The BSA adsorption amount on the membranes was calculated by measuring the initial and final BSA concentrations of the adsorption media. The BSA concentration was then determined through a bicinchoninic acid assay (BCA) using a Pierce BCATM Protein Assay Kit²⁷. To study the reusability of the NCNFs, one piece (about 10 mg) of nanofibrous membrane with a known amount of adsorbed BSA was immersed in 20 mL of 1 M NaSCN solution as elution medium for 1 h at 30 °C. The amount of the eluted BSA was determined by measuring the concentration of BSA in the elution through BCA. This BSA adsorption–elution process was repeated ten times with the same nanofibrous membranes.

3. Results and discussion

3.1. Fabrication of NCNFs

During solution blowing, spinning solutions are blown and attenuated into ultrafine

fibers by a high-velocity airflow, along with evaporation of the solvent. In this work, the coaxial solution-blowing apparatus was designed with a coaxial spinneret to allow two spinning solutions to coaxially extrude into the high-velocity airflow field to form the core-shell nanofibers. To study the effect of the ratio of core and shell components on fiber morphology, the fibers with different core-shell injection speed ratio (core-shell ratio was 1:2, 1:1, 2:1, respectively) was confirmed by TEM, as shown in Fig. 1. The images clearly show the presence of a continuous core material inside the nanofibers. Distinct interfaces between the core and shell components are also evident, which indicates that nylon-6 was completely encapsulated inside the fiber. The images also suggest that the thickness of the shell layer can be adjusted by controlling the injection speed of the shell and core solutions.

The surface morphologies of the nanofibers are shown in Fig. 2(a-j). The images reveal that the solution-blown nanofibers were arranged disorderly and formed three-dimensional mats. The nanofibers were smooth in surface and curly in shape, with diameters ranging from 80 nm to 650 nm. When chitosan solution was used solely as the shell spinning solution (Fig. 2a), the nanofibers produced were small in diameter with many droplets along the fibers. Chitosan solution is difficult to spin by this process because of its high viscosity even at low concentrations¹⁵. Hence, in this work, PVA was blended with chitosan as an assistant polymer to enhance the latter's spinnability and confer good water absorption capability to the nanofibers. Addition of PVA made the spinning process smooth and promoted the gradual disappearance of droplets with increasing PVA content (Figs. 2a-d, 2i, and 2j). By contrast, addition of

EGDE (Figs. 2d, 2g, and 2h) caused no apparent change in the fibers.

3.2. CB immobilization

CB is a popular affinity dye ligand for the purification of protein molecules. In this work, CB was immobilized onto the nanofiber surface to enhance the adsorption capacity of the latter. The CB-immobilized NCNFs (NCNFs-co-CB) was observed by SEM; the image was shown in Fig. 2k. Good stability in shape was observed with a slight increase in diameter for the NCNFs-co-CB. Attenuated total reflectance (ATR)-FTIR was used to study the chemical structure changes. Fig. 3 shows the main adsorption peaks of CB molecules on the membranes. The peaks at 1086, 1144, and 1248 cm^{-1} correspond to the stretching vibrations of S=O, respectively²⁸⁻²⁹. Compared with the pristine NCNFs, the two characteristic adsorption peaks on NCNFs-co-CB membranes confirm the presence of CB molecules on the nanofibrous membranes. This result was obtained because NCNFs-co-CB was prepared through a nucleophilic reaction between the CB triazinyl chloride and the abundant hydroxyl groups on the NCNF surface, as shown in Fig. 4³⁰.

The CB amount immobilized on the nanofibrous membrane was determined by the sulfur content using EA. In this process, only the shell material (PVA and chitosan) was used to calculate the amount of the immobilized CB, as shown in Fig. 5. The figure indicates that the amount of immobilized CB increased with increasing PVA ratio, but decreased with EGDE content (i.e., increasing degree of cross-linking). This observation may have occurred because CB was immobilized mainly through a nucleophilic reaction between the CB triazinyl chloride and abundant hydroxyl groups

of the NCNF surfaces³⁰.

3.3. BSA adsorption

BSA is widely used as a protein model because of its similar molecular weight range to many proteins and enzymes and its low cost compared with other biological agents. In addition, CB and BSA can form a ligand–ligate pair, which has also been used frequently for affinity chromatography³¹. In this work, BSA adsorption behavior to the membranes were studied to evaluate the effects of shell content, adsorption time, initial BSA concentration, and pH value on membrane binding.

The BSA adsorption performances of different contents of the samples were studied and results shown in Fig. 6. By comparing all of the pristine NCNFs, we noted that PVA content greatly influences BSA adsorption capacity. In particular, the absence of PVA in the shell material (NCNFs-1), yielded a BSA adsorption capacity of 154.83 mg/g only. With increasing PVA content, the adsorption was augmented; the highest adsorption occurred at chitosan:PVA = 50:50 (the BSA adsorption of pristine NCNFs is 276.16 mg/g). After CB was immobilized on the surface, the adsorption capacity of the NCNF further improved. As mentioned earlier, the amount of immobilized CB increases with increasing PVA ratio. Hence, CB and PVA react synergistically to enhance the adsorption capacity of NCNFs-co-CB significantly. For instance, the adsorption capacity of BSA to NCNFs-5 increased from 276.16 mg/g to 379.43 mg/g after CB immobilization. Introduction of PVA to the shell improved the adsorption capacity of BSA, which can be attributed to the abundant hydroxyl groups along the PVA macromolecular chain. These hydroxyl groups act as adsorption sites and

contribute to the hydrogel property, which increases the effective surface area as the nanofibers swell in aqueous condition. EGDE contents showed a different effect. By comparing the results from NCNFs-8, NCNFs-4, and NCNFs-7, we found that the nanofibers adsorbed less BSA with increasing EDGE content. EDGE contains two epoxide groups at both ends of its molecular chain, which could react mainly with $-OH$ groups after cross-linking. Overall, comprehensive evaluation of the performances of the membranes, including spinnability and adsorption properties, indicated that the NCNFs-5 membrane is superior to all other membranes tested in this study. Subsequently, the adsorption performance of NCNFs-5 was further examined to determine the effect of adsorption time, initial BSA concentration, and pH value to membrane adsorption.

As seen in Fig. 7, the amount of adsorbed BSA on NCNFs and NCNFs-co-CB increased significantly in the first 7 h up to 276.14 mg/g and 379.32 mg/g nanofiber, respectively, until equilibrium was reached after 10 h.

Fig. 8 shows the influence of initial BSA concentration on NCNF adsorption performance. At a fixed adsorption time of 10 h, the amount of BSA adsorbed onto the NCNFs and NCNFs-co-CB increased with increasing initial BSA concentration. The trend plateaued at an initial BSA concentration of about 3 mg/mL. At this point, the BSA adsorption capacities of NCNFs and NCNFs-co-CB were 276.08 and 379.19 mg/g nanofiber, respectively.

The influence of pH on NCNF adsorption performance was studied and the effect of pH was investigated at the pH range of 4.0–9.18 using different buffers. It

presented that pH value had a significant effect on the adsorption performance of BSA (Fig. 9). The figure shows that the BSA adsorption was relatively large at pH 6-7, and the maximum BSA adsorption capacity of the NCNFs-co-CB was observed at pH 7.14. As we all know, electrostatic interactions to charged BSA molecules play important role in the BSA adsorption³². Chitosan is a kind of polyelectrolyte with pK_a around 6.5 which exhibits a pH-sensitive behavior as a weak polymer due to the amino groups on its chain³³. Therefore, chitosan is positive charged at near or below the neutral pHs which can offer binding sites for BSA²³. In addition, conformational changes in the protein molecules adsorbed on the PVA particles and from dye attachment also impact on pH-responsive³⁴. This behavior is consistent with the results shown in Fig. 9.

4. Conclusions

Nylon-6 core–chitosan/PVA shell nanofibers (NCNFs) were fabricated through a novel solution-blowing process. NCNFs-co-CB which immobilized CB on the NCNFs possesses the advantages of both hydrogel and fibers mats and exhibits a high adsorption capacity. The NCNFs with the ratio of core/shell is 1:2, chitosan: PVA = 50:50 at pH 7.14 and 37 °C showed the best BSA adsorption capacity among all the samples. These results suggest that the NCNF is a highly suitable and promising affinity adsorption material.

Acknowledgements

The author would like to thank National Natural Science Foundation of China

(51473121), Tianjin Natural Science Foundation (13JCZDJC32600) and Technology program of Tianjin Municipal Education Commission (20130313) for their financial support.

References

- 1 N. B. Iannucci, F. J. Wolman, S. A. Camperi, A. A. Navarro del Canizo, M. Grasselli and O. Cascone. Affinity chromatography with pseudobiospecific ligands on high-performance supports for purification of proteins of biotechnological interest. *Br J. Chem. Eng.*, 2003, 20, 27-32.
- 2 A. F. Che, X. J. Huang and Z. K. Xu, Polyacrylonitrile-based nanofibrous membrane with glycosylated surface for lectin affinity adsorption, *J. Membr. Sci.*, 2011, 366, 272-277.
- 3 E. Klein, Affinity membranes: a 10-year review, *J. Membr. Sci.*, 2000, 179, 1-27.
- 4 C. Charcosset, Purification of proteins by membrane chromatography, *J. Chem. Technol. Biotechnol.* 1998, 71, 95-110.
- 5 D. Li, Y. Xia, Electropinning of nanofibers: reinventing the wheel? *Adv. Mater.* 2004, 16, 1151-1170.
- 6 Z. Ma, M. Kotaki and S. Ramakrishna, Electrospun cellulose nanofiber as affinity membrane, *J. Membr. Sci.*, 2005, 265, 115-123.
- 7 A. Greiner, J. H. Wendorff, Electrospinning: a fascinating method for the preparation of ultrathin fibres, *Angew. Chem. Int. Ed.*, 2007, 46, 5670-5703.
- 8 V. Karako, H. Yavuz and A. Denizli, Affinity adsorption of recombinant human

interferon- α on a porous dye-affinity adsorbent, *Physicochem. Eng. Aspects*, 2004, 240, 93-99.

9 L.R. Castilho, F.B. Anspach and W.D. Deckwer, Comparison of affinity membranes for the purification of immunoglobulins, *J. Membr. Sci.*, 2002, 207, 253-264.

10 H. Y. Liu, Y. Zheng and P. V. Gurgel, Carbonell, Affinity membrane development from PBT nonwoven by photo-induced graft polymerization, hydrophilization and ligand attachment, *J. Membr. Sci.*, 2013, 428, 562-575.

11 C. Boss, E. Meurville, J. M. Sallese and P. Ryser, Size-selective diffusion in nanoporous alumina membranes for a glucose affinity sensor. *J. Membr. Sci.*, 2012, 401-402, 217-221.

12 H. X. Sun, L. Zhang, H. Chai, J. Yu, H. Qian and H. L. Chen, A study of human-globulin adsorption capacity of PVDF hollow fiber affinity membranes containing different amino acid ligands, *Sep. Purif. Technol.*, 2006, 48, 215-222.

13 H. T. Zhang, C. Y. Wu and Y. L. Zhang, Elaboration, characterization and study of a novel affinity membrane made from electrospun hybrid chitosan/nylon-6 nanofibers for papain purification, *J. Mater. Sci.*, 2010, 45, 2296-2304.

14 Z. W. Ma, S. Ramakrishna, Electrospun regenerated cellulose nanofiber affinity membrane functionalized with protein A/G for IgG purification, *J. Membr. Sci.*, 2008, 319, 23-28.

15 X. P. Zhuang, X. C. Yang, L. Shi, B. W. Cheng, K. T. Guan and W. M. Kang, Solution blowing of submicron-scale cellulose fibers, *Carbohydr. Polym.*, 2012, 90, 982-987.

- 16 L. Shi, X. P. Zhuang, X. X. Tao, B. W. Cheng and W. M. Kang, *Fibers and Polymers-Solution Blowing Nylon 6 Nanofiber Mats for Air Filtration*, *Fiber Polym.*, 2013, 14, 1485-1490.
- 17 X. P. Zhuang, K. F. Jia, B. W. Cheng, X. Feng, S. J. Shi and B. Zhang, *Solution blowing of continuous carbon nanofiber yarn and its electrochemical*, *Chem. Eng. J.*, 2014, 237, 308-311.
- 18 X. X. Tao, G. Q. Zhou, X. P. Zhuang, B. W. Cheng, X. J. Li and H. J. Li, *Solution blowing of activated carbon nanofibers for phenol adsorption*, *RSC Adv.*, 2015, 5, 5801-5808.
- 19 X. L. Xu, L. Li, H. Wang, X. J. Li and X. P. Zhuang, *Solution blown sulfonated poly(ether ether ketone) nanofiber-Nafion composite membranes for proton exchange membrane fuel cells*, *RSC Adv.*, 2015, 5, 4934-4940.
- 20 X. P. Zhuang, L. Shi, K. F. Jia, B. W. Cheng and W. M. Kang, *Solution blown nanofibrous membrane for microfiltration*, *J. Membr. Sci.*, 2013, 429, 66-70.
- 21 H. Esfahani, M. P. Prabhakaran, E. Salahi, A. Tayebifard, M. Keyanpour-Rad, M. R. Rahimipour and S. Ramakrishna, *Protein adsorption on electrospun zinc doped hydroxyapatite containing nylon 6 membrane: Kinetics and isotherm*, *J. Colloid Interf. Sci.*, 2015, 443, 143-152.
- 22 C. L. Bell, N. A. Peppas, *Biomedical membranes from hydrogels and interpolymer complexes*, *Adv. Polym. Sci.*, 1995, 22, 125-176.
- 23 S. Mondal, C. Li and K. Wang, *Bovine Serum Albumin Adsorption on Glutaraldehyde Cross-Linked Chitosan Hydrogels*, *J. Chem. Eng. Data*, 2015, 60,

2356-2362.

24 R. F. Liu, X. L. Xu, X. P. Zhuang and B. W. Cheng, Chitosan/PVA hydrogel nanofiber mats, *Carbohydr. Polym.*, 2014, 101, 1116-1121.

25 L. Chiappisi, M. Gradzielski, Co-assembly in chitosan-surfactant mixtures: Thermodynamics, structures, interfacial properties and applications, *Adv. Colloid Interface*, 2015, 220, 92-107.

26 C. Risdian, M. Nasir, A. Rahma and H. Rachmawati, The Influence of Formula and Process on Physical Properties and the Release Profile of PVA/BSA Nanofibers Formed by Electrospinning Technique, *J. Nano. Res.*, 2015, 31, 103-113.

27 P. K. Smith, R. I. Krohn, G. T. Hermanson, A. K. Mallia, F. H. Gartner, M. D. Provenzano, E. K. Fujimoto, N. M. Goeko, B. J. Olson and D. C. Klenk, Measurement of protein using bicinchoninic acid, *Anal. Biochem*, 1985, 150, 76-85.

28 S. Akgol, N. Tuzmen and A. Denizli, Porous dye affinity beads for albumin separation from human plasma, *J. Appl. Polym. Sci.* 2007, 105, 1251-1260.

29 M. C. Martins, E. Naeemi, B. Ratner and M. A. Barbosa, Albumin adsorption on Cibacron Blue F3GA immobilized onto oligo(ethylene glycol)-terminated self assembled monolayers, *J. Mater. Sci.: Mater. Med.*, 2003, 14, 945-954.

30 J. Zhu, J. Yang and G. Sun, Cibacron Blue F3GA functionalized poly(vinyl alcohol-co-ethylene) (PVA-co-PE) nanofibrous membranes as high efficient affinity adsorption materials, *J. Membr. Sci.*, 2011, 385-386, 269-276.

31 Z. W. Ma, K. Masaya and S. Ramakrishna, Immobilization of Cibacron Blue F3GA on electrospun polysulphone ultrafine fiber surfaces towards developing an

affinity membrane for albumin adsorption, *J. Membr. Sci.*, 2006, 282, 237-244.

32 J. Zhang, Z. Zhang, Y. Song, H. Cai, Bovine serum albumin (BSA) adsorption with Cibacron Blue F3GA attached chitosan microspheres, 2006, 66, 916-923

33 F. Cuomo, F. Lopez, A. Ceglie, L. Maiuro, M. G. Miguelb and B. Lindman, pH-responsive liposome-templated polyelectrolyte nanocapsules, *Soft Matter.*, 2012, 8, 4415-4420.

34 A. Denizli, A. Tuncel, A. Kozluca, K. Ecevit and E. Piskin, Cibacron Blue F3GA attached poly(vinyl alcohol) particles for specific albumin adsorption, *Sep. Sci. Technol.*, 1997, 32, 1003-1015.

Table caption:

Table 1. The experimental scheme.

Figure captions:

Fig. 1. TEM images of the solution-blown core-shell nanofibers. (a) NCNFs-5, (b) NCNFs-4, and (c) NCNFs-6.

Fig. 2. SEM images of solution-blown NCNFs. (a) NCNFs-1, (b) NCNFs-2, (c) NCNFs-3, (d) NCNFs-4, (e) NCNFs-5, (f) NCNFs-6, (g) NCNFs-7, (h) NCNFs-8, (i) NCNFs-9, (j) NCNFs-10, and (k) NCNFs-co-CB.

Fig. 3. ATR-FTIR spectra of (a) CB, (b) pristine NCNF and (c) NCNF-co-CB.

Fig. 4. CB immobilization onto NCNFs.

Fig. 5. The immobilized amount of CB on NCNFs.

Fig. 6. BSA adsorption of nanofibers.

Fig. 7. Effect of adsorption time on BSA adsorption capacity to NCNFs and NCNFs-co-CB (pH: 7.14, T: 37 °C, and initial BSA concentration: 3 mg/mL).

Fig. 8. Effect of initial BSA concentration on the BSA adsorption capacity of NCNFs and NCNFs-co-CB (pH: 7.14, temperature: 37 °C, and adsorption time: 10 h).

Fig. 9. Effect of pH on the BSA adsorption capacity of NCNFs-co-CB (Temperature: 37 °C, adsorption time: 10 h, and initial BSA concentration: 3 mg/mL).

Table.1. The experimental scheme

Samples	Shell material (chitosan:PVA)	Content of EGDE*	Injection speed (core:shell)
NCNFs-1	100:0	10%	1:1
NCNFs-2	80:20	10%	1:1
NCNFs-3	60:40	10%	1:1
NCNFs-4	50:50	10%	1:1
NCNFs-5	50:50	10%	1:2
NCNFs-6	50:50	10%	2:1
NCNFs-7	50:50	20%	1:1
NCNFs-8	50:50	5%	1:1
NCNFs-9	40:60	10%	1:1
NCNFs-10	20:80	10%	1:1

*EGDE content is expressed as percent weight with respect to the total chitosan and PVA content.

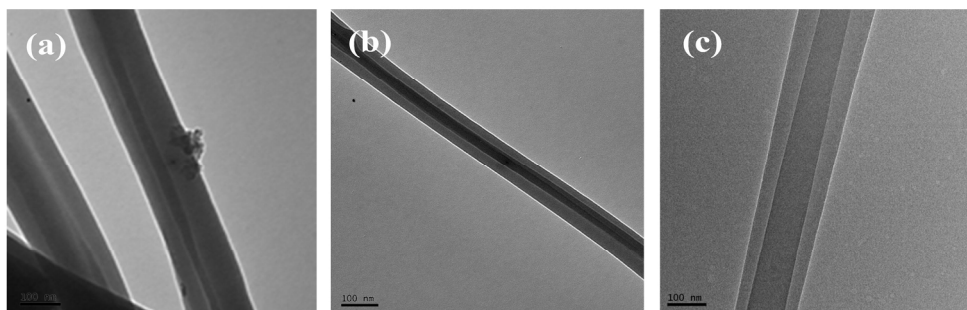


Fig. 1. TEM images of the solution-blown core-shell nanofibers. (a) NCNFs-5, (b) NCNFs-4, and (c) NCNFs-6. 200x68mm (300 x 300 DPI)

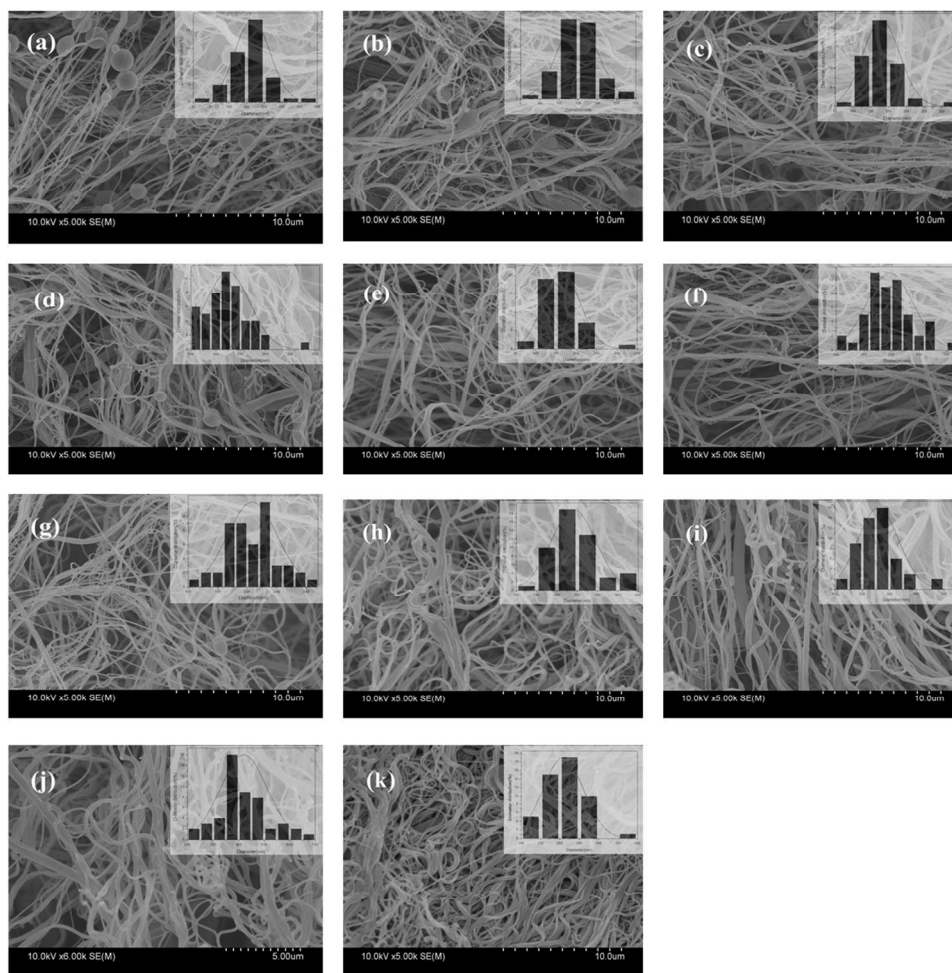


Fig. 2. SEM images of solution-blown NCNFs. (a) NCNFs-1, (b) NCNFs-2, (c) NCNFs-3, (d) NCNFs-4, (e) NCNFs-5, (f) NCNFs-6, (g) NCNFs-7, (h) NCNFs-8, (i) NCNFs-9, (j) NCNFs-10, and (k) NCNFs-co-CB. 104x105mm (300 x 300 DPI)

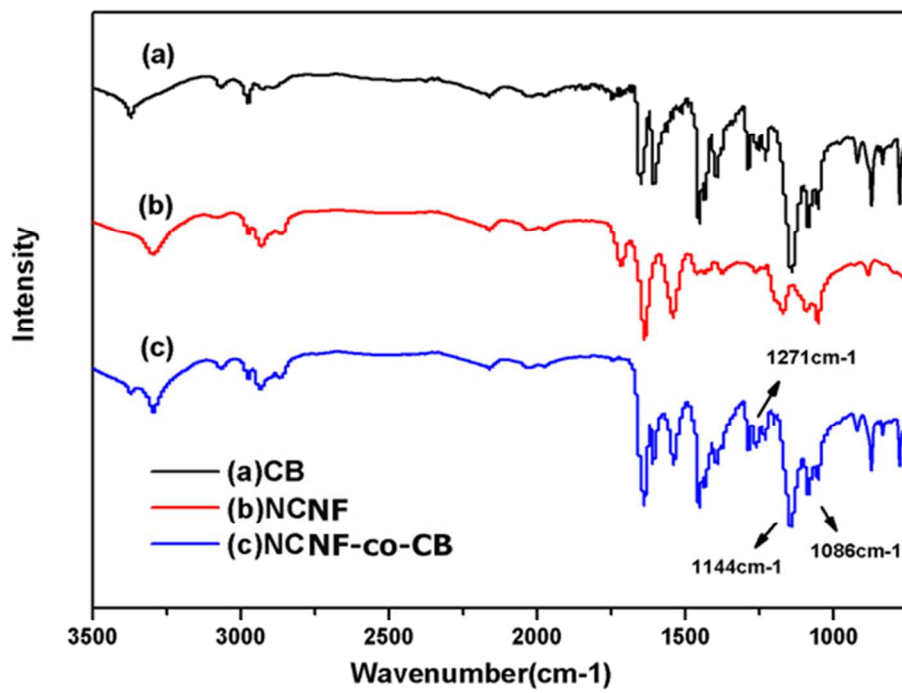


Fig. 3. ATR-FTIR spectra of (a) CB, (b) pristine NCNF and (c) NCNF-co-CB.
55x43mm (300 x 300 DPI)

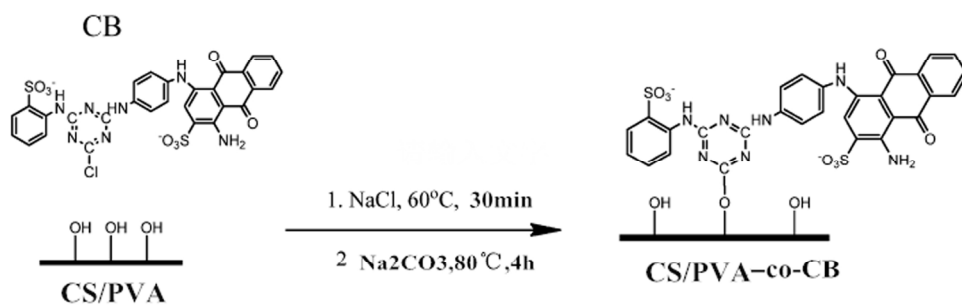


Fig. 4. CB immobilization onto NCNFs.
200x80mm (300 x 300 DPI)

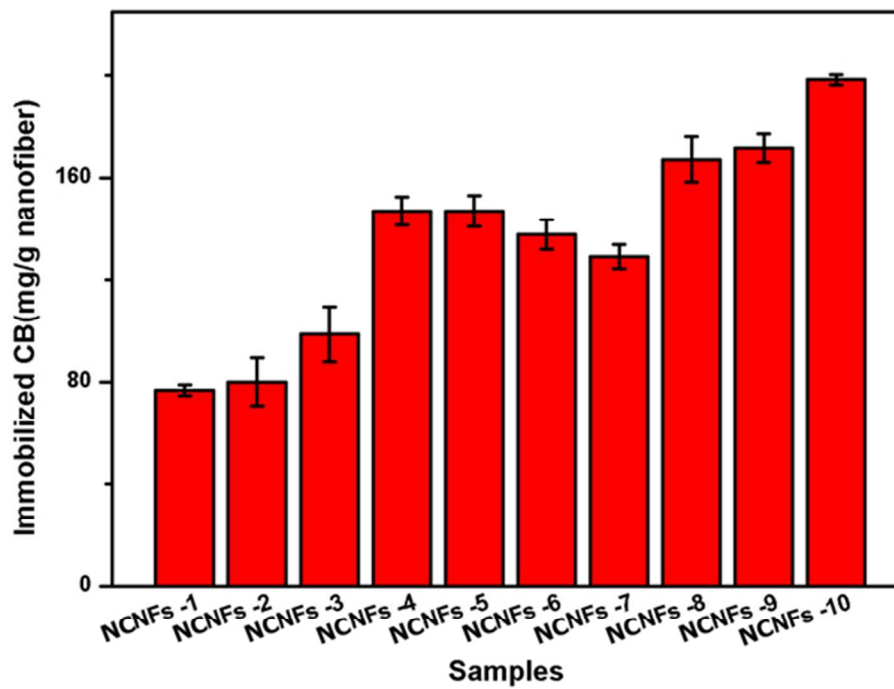


Fig. 5. The immobilized amount of CB on NCNFs.
56x45mm (300 x 300 DPI)

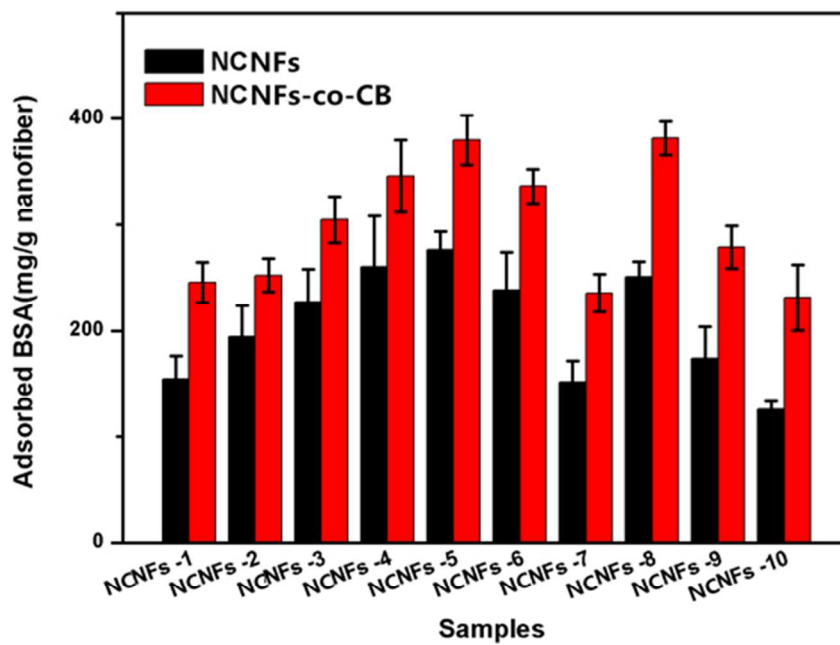


Fig. 6. BSA adsorption of nanofibers.
56x42mm (300 x 300 DPI)

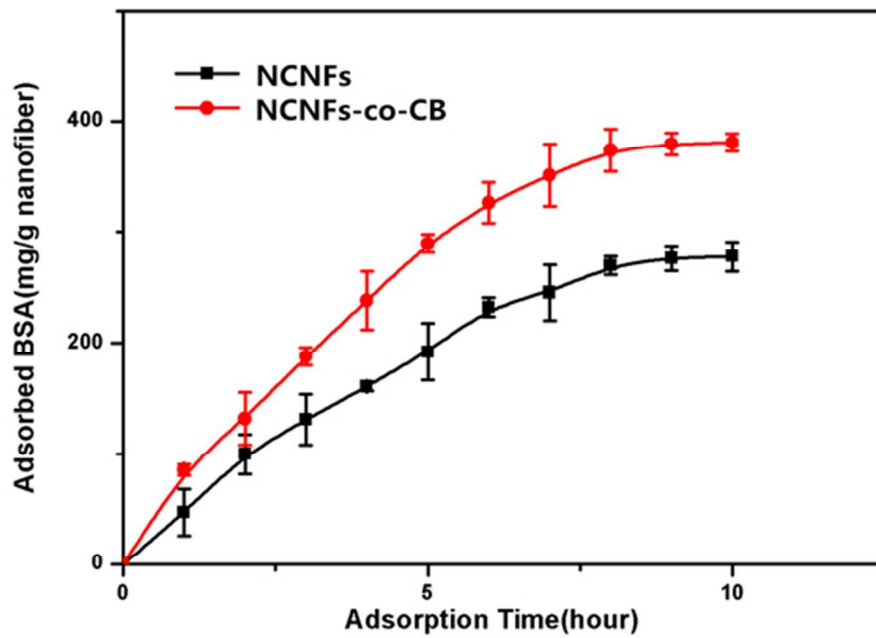


Fig. 7. Effect of adsorption time on BSA adsorption capacity to NCNFs and NCNFs-co-CB (pH: 7.14, T: 37 °C, and initial BSA concentration: 3 mg/mL).
53x38mm (300 x 300 DPI)

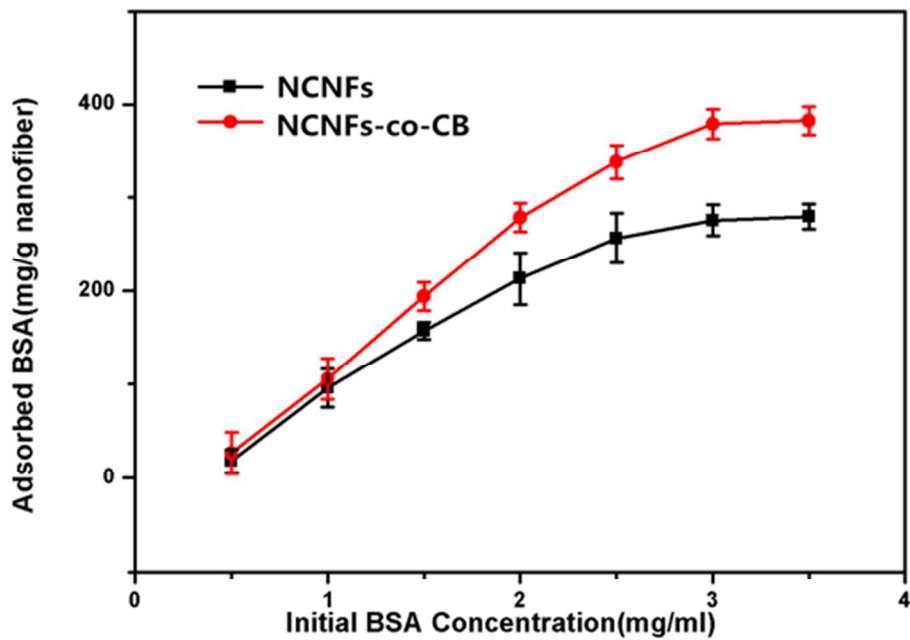


Fig. 8. Effect of initial BSA concentration on the BSA adsorption capacity of NCNFs and NCNFs-co-CB (pH: 7.14, temperature: 37 °C, and adsorption time: 10 h).
53x39mm (300 x 300 DPI)

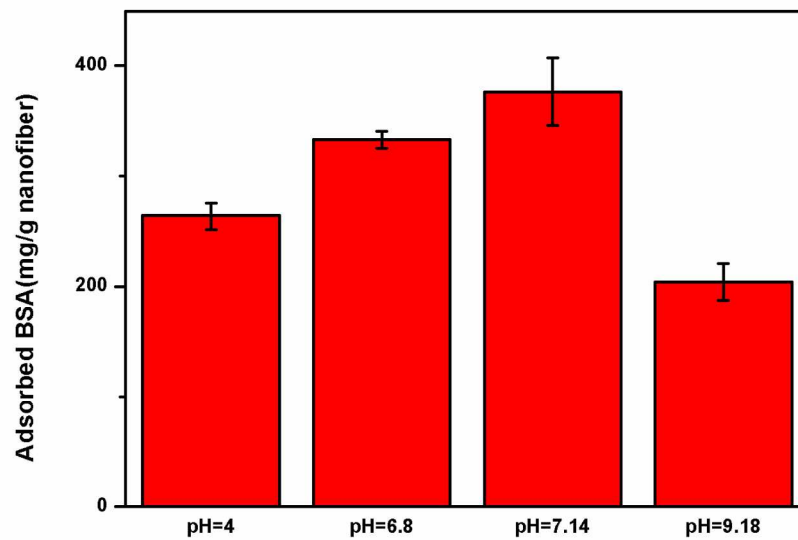


Fig. 9. Effect of pH on the BSA adsorption capacity of NCNFs-co-CB (Temperature: 37 °C, adsorption time: 10 h, and initial BSA concentration: 3 mg/mL).
200x132mm (300 x 300 DPI)